Available online at www.sciencedirect.com
ScienceDirect
Catalysis Today 131 (2008) 82–89
CATALYSIS TODAY
www.elsevier.com/locate/cattod

Direct synthesis and catalytic performance of ultralarge pore GaSBA-15 mesoporous molecular sieves with high gallium content

M. Selvaraj, S. Kawi *

Department of Chemical and Biomolecular Engineering, National University of Singapore, Singapore 119260

Available online 21 December 2007

Abstract

Mesoporous GaSBA-15 molecular sieves with different n_{Si}/n_{Ga} ratios have been directly synthesized using Pluronic 123 triblock polymer as a structure-directing agent by pH-adjusting method. The mesoporous materials have been characterized using ICP-AES, XRD, N_2 adsorption, ^{71}Ga-MAS NMR, SEM and TEM. ICP-AES studies show a high amount of gallium incorporation on the silica pore walls. The structural and textural properties of calcined GaSBA-15 are characterized by XRD and N_2 adsorption. ^{71}Ga MAS NMR results demonstrate that a high amount of tetrahedral-gallium could be substituted for Si in the framework of SBA-15. TEM and FE-SEM images show the uniform pore diameter and rope-like hexagonal mesoporous structure of GaSBA-15. These GaSBA-15 materials have been used as catalysts for vapour-phase *t*-butylation of 1,2-dihydroxybenzene (DHB) for selective synthesis of 4-*t*-butylcatechol (4-TBC) under different reaction conditions. GaSBA-15(10) gave the highest 93.2% conversion of DHB and 95.7% selectivity of 4-TBC as compared with other GaSBA-15 catalysts.

Keywords: Direct hydrothermal synthesis; GaSBA-15; pH-adjusting method; *t*-Butylation of DHB; Conversion of DHB; Selectivity of 4-TBC

1. Introduction

Alkylation of hydroxyaromatic derivatives to prepare alkyl-substituted phenols is an important fine chemical catalytic reaction process as alkyl-substituted phenols are used as raw materials for the synthesis of polymer stabilizers, antioxidants, intermediates in the manufacture of value added chemicals, such as pharmaceuticals and agro chemicals. *t*-Butylation of DHB is an industrially important reaction, and 4-TBC is an important product of this reaction. 4-TBC and its derivatives are used as raw materials for the synthesis of several polymerization inhibitors, dye developers, pharmaceuticals, and agricultural chemicals. Commercial alkylation of aromatics is carried out via electrophilic substitution, where Lewis acids, such as $AlCl_3$, $ZnCl_2$, HCl and H_2SO_4, are the most commonly available catalysts [1]. In a Japanese patent [2], 4-TBC was prepared from DHB and *t*-butylalcohol in the presence of Friedel–Crafts type catalysts, $ZnCl_2$, $FeCl_3$, and HCl, with low conversion and selectivity. In other patents [3,4], di-*t*-butylation of hydroquinone was achieved by isobutene over acidic resin with low conversion and selectivity [5]. The use of these catalysts gives rise to many problems concerning handling, safety, corrosion, and waste disposal. Much effort has been put into developing an alternative technology based on heterogeneous catalysts [6]. The use of zeolites in organic reactions has grown over the last several years because of the shape selectivity, which zeolites impose on a reaction, together with lower environment pollution and higher purity of the product [7,8]. Hence, many reports on the aromatics alkylation over solid acid catalysts with alcohol or olefin as an alkylating agent have been published [9–11], reporting parameters which affect catalytic properties.

Although many articles about aromatics alkylation have been reported, however, only a few patents [2–4] and papers [12] on the butylation of dihydroxy-substituted aromatics have been disclosed until now. Recently, literatures have reported the *t*-butylation of 1,2-dihydroxybenzene (DHB) with *t*-butylalcohol over zeolites [12]. From the above solid acid catalysts, low yield and selectivity of *para* isomer is obtained because their catalytic performances were limited by diffusional constraints associated with different type of pores [13]. Moreover, the need for present day heterogeneous catalysts in processing hydrocarbons with high molecular weights has led researchers to

* Corresponding author.
E-mail address: chekawis@nus.edu.sg (S. Kawi).

0920-5861/$ – see front matter © 2007 Published by Elsevier B.V.
doi:10.1016/j.cattod.2007.10.046

search for better catalyst systems. These limitations could be overcome by mesoporous Al-MCM-41 materials [14,15], which have highly-ordered mesopores, large surface area, high thermal stability and mild acidity; these unique properties render the possibility of applying these mesoporous Al-MCM-41 materials as solid acid catalysts in the alkylation of large molecules. For an instance, Selvaraj et al. recently used Zn–Al-MCM-41 catalysts for *t*-butylation of DHB [16].

The discovery of ordered mesoporous materials has sparked great interest owing to their potential applications in catalysis, in adsorption and separation processes, and as support for nanostructured materials with novel physical and chemical properties. In 1998, a new synthesis pathway to large-pore mesoporous SBA-15 materials was found in which triblock copolymers act as structure-directing agents [17]. The mesoporous materials exhibit larger pore size, thicker pore wall and better hydrothermal stability compared with M41S; however, SBA-15 could not be directly used as a catalyst due to the lack of acidity. Therefore, only a few papers reported the use of metal-substituted SBA-15 as catalysts for alkylation reactions, especially the synthesis, characterization and application of GaSBA-15 [18].

In the present study, GaSBA-15 catalysts have been synthesized and used as catalysts for the selective synthesis of 4-TBC by *t*-butylation of DHB using isobutene as the alkylating reagent. The effect of different catalysts, reaction temperature, WHSV, and isobutene to DHB molar ratio on the selectivity of 4-*t*-butylcatechol and regenerability of the catalyst has been investigated.

2. Experimental

2.1. Synthesis of GaSBA-15

Mesoporous GaSBA-15 materials were synthesized using pH-adjusting method according to a recently published procedure for the synthesis of CrSBA-15 [19]. In a typical synthesis of GaSBA-15, 4 g of Pluronic P123 – used as a template – was dissolved in 25 mL of water to get a clear solution with pH <1.6. In order to adjust the pH of this solution above 1.8, 75 mL of 0.25 M HCl solution with n_{H_2O}/n_{HCl} ratio of 295 was added to the solution and the solution mixture was again stirred for another 1 h in order for the hydronium ions to be associated with the alkylene oxide units. Then, 9 g of tetraethyl orthosilicate together with the required amount of gallium nitrate hydrate solution (to yield GaSBA-15 with n_{Si}/n_{Ga} = 10, 15, 25, and 50) were added to the solution mixture, yielding a gel-like solution with pH >2. The resulting mixture was again stirred for 24 h at 313 K before it was transferred into an autoclave to be hydrothermally treated at 373 K for 24 h. After hydrothermal process, the solid products were recovered by filtration, washed several times with water, and dried overnight at 373 K. The molar composition of the gel was 1 TEOS/0.02–0.1 Ga_2O_3/0.016 P123/0.43–5.2 HCl/127–210 H_2O. Finally, the samples were calcined at 813 K in air for 6 h for complete removal of the template.

2.2. Characterization

The elemental composition of the resultant solid products was analysed by ICP-AES (Perkin Elmer, Optima 3000) after the samples were dissolved in a HF solution. The small-angle XRD patterns were recorded under ambient conditions on a Shimadzu XRD-6000 with Cu Kα radiation (λ = 1.5406 Å). The X-ray tube was operated at 40 kV and 30 mA while the diffractograms were recorded in the 2θ range of 0.6–5° with a 2θ step size of 0.01° and a step time of 10 s.

Nitrogen adsorption/desorption measurements were conducted using Quantachrome Autosorb-1 by N_2 physisorption at 77 K. All samples were outgassed for 3 h at 250 °C under vacuum ($p < 10^{-5}$ hPa) in the degas port of the sorption analyzer. The BET specific surface areas of the samples were calculated in the range of relative pressures between 0.05 and 0.35. The pore size distributions were calculated from the adsorption branch of the isotherm using the thermodynamics-based Barrett–Joyner–Halenda (BJH) method. The total pore volume was determined from the adsorption branch of the N_2 isotherm at p/p_0 = 1. The pore wall thickness (t_w) was calculated from the unit cell parameter (a_0) and pore diameter (d_p).

^{71}Ga spectra were recorded at 11.75 T on a Varian INOVA 500 NMR spectrometer with CPIMS probe. ^{71}Ga spectra were acquired at 152.5 MHz with 8.0 μs pulse length, recycling time 1.000 s, and a SiN rotor 5 mm in diameter without spinning and with spinning at 10 kHz. The chemical shifts were given in ppm; for ^{71}Ga NMR, usually 1 M aqueous $Ga(NO_3)_3$ solution was chosen as the external reference sample to determine the signal position of $\delta([M(H_2O)_6]^{3+}) = 0$ ppm. All spectra were recorded at room temperature.

Field emission-scanning electron microscopy (FE-SEM) images were obtained with a JEOL JSM-6700F microscope at an accelerating voltage of 5.0 kV. Transmission electron microscopy (TEM) images were collected on a JEOL 2010 electron microscope operated at an acceleration voltage of 200 kV.

2.3. Catalytic studies

The catalytic alkylation of DHB (Aldrich 99+%) with isobutene was carried out with different reaction temperature at atmospheric pressure using a fixed-bed vertical flow reactor. Different molar ratios of isobutene/DHB were introduced into the reactor with various WHSV (h^{-1}). The liquid products were collected at different times, and analyzed by gas chromatography using a flame ionization detector and SE-30 30 m capillary column. Reaction products were identified by GC/MS (HP 5890 II GC–HP 5971 Mass Selective Detector) and ^{1}H NMR (GEMINI-2000, 200 MHz).

2.4. Recyclability

The used GaSBA-15 catalyst was calcined at 500 °C in air for the removal of unreacted reactants and coke formation, and then the catalyst again was reused for the catalytic alkylation of DHB reaction.

3. Results and discussion

3.1. Formation of GaSBA-15

Mesoporous GaSBA-15 synthesized under highly acidic condition (pH <1) has a low amount of Ga incorporated into SBA-15, possibly due to the high solubility of gallium precursors, which hinder their incorporation into the silica walls of SBA-15. However, the hydrolysis rate of both TEOS, which is used as the silica precursor, and gallium nitrate hydrate, which is used as the gallium precursor, may not be equally matched each other. Therefore, an attempt to increase the amount of Ga-ions (n_{Si}/n_{Ga} ratio = 10 in gel) incorporated in the framework has been done in this study by simply adjusting the gel pH using the aqueous HCl solution prepared with n_{H_2O}/n_{HCl} molar ratio of 295 without changing the structural integrity of the parent SBA-15 materials.

The synthesis mechanism is explained as follows: The hexagonal phase is initially formed by adjusting the pH of the synthesis gel between 0 and 1.6. Once the surfactant and silica species have been protonated, the cationic silica species undergo partial condensation and form mesostructure through the counteranion (X^-) with the cationic surfactant species; as a result, the pH of the synthesis medium increases. When the pH of the synthesis gel is still high at 1.8 even after the addition of the silicon source and a few hours of stirring, the Ga precursor is then added while the pH of the synthesis gel is adjusted by aqueous HCl solution (n_{H_2O}/n_{HCl} molar ratio = 295) to around 2.2, which is above the zero net charge of silica. If the pH of the synthesis medium rises above the zero net charge of silica, the silica species are negatively charged, thus enhancing the interaction with the $Ga(OH)_2^+$ species. With decreasing H^+ concentration in the synthesis gel, the concentration of gallium hydroxyl species increases. Hence, the partially condensed silica species are able to form Ga–O–Si bond with $Ga(OH)_2^+$ species at high pH. Moreover, the structural order of the mesoporous material is maintained when it is formed at a pH of ca. 2.2. The synthesised GaSBA-15 materials have been characterized by ICP-AES, XRD, N_2 adsorption, ^{71}Ga MAS NMR, FE-SEM, and TEM as follows.

3.2. XRD

The powder XRD patterns of calcined GaSBA-15 samples with different n_{Si}/n_{Ga} ratios are shown in Fig. 1. The well-defined XRD patterns are similar to those recorded for silica SBA-15 materials as described by Zhao et al. [17]. The XRD patterns of all GaSBA-15 materials exhibit three well-resolved peaks which are indexed to the (1 0 0), (1 1 0), and (2 0 0) reflections of the high crystallinity-hexagonal space group *p6mm,* and the XRD peaks are observed to shift to lower angle with increasing Ga-content. The unit cell parameter a_0 is calculated from $a_0 = 2d_{100}/\sqrt{3}$, where the d-spacing values are calculated by $n\lambda = 2d\sin\theta$. The observed d spacings and unit cell parameter results are well-matched with the hexagonal *p6mm* space group. When the n_{Si}/n_{Ga} molar ratio are gradually decreased from 50 to 10, the size of the unit cell a_0 increases from 119.4 to 123.7 Å due to the increase of the amount of Ga-ions incorporated on the silica pore walls. This is because the Ga–O bond length is higher than the Si–O bond length due to the larger ionic radius of Ga than Si, hence increasing the repeat distance in GaSBA-15; however, the Ga–O–Si bond angle decreases with increasing gallium content. The effects of increasing bond length and decreasing bond angle play dominating roles in the variations of repeat distances. Moreover, it is found through ICP-AES analysis that the n_{Si}/n_{Ga} ratio of the calcined GaSBA-15 decreases from 85.3 to 12.7 with n_{H_2O}/n_{HCl} molar ratio of 295. The above described experimental results suggest that the pH-adjusting method is necessary for a high amount of Ga-ion incorporation on the silica pore walls without affecting the structural order of the parent SBA-15 materials.

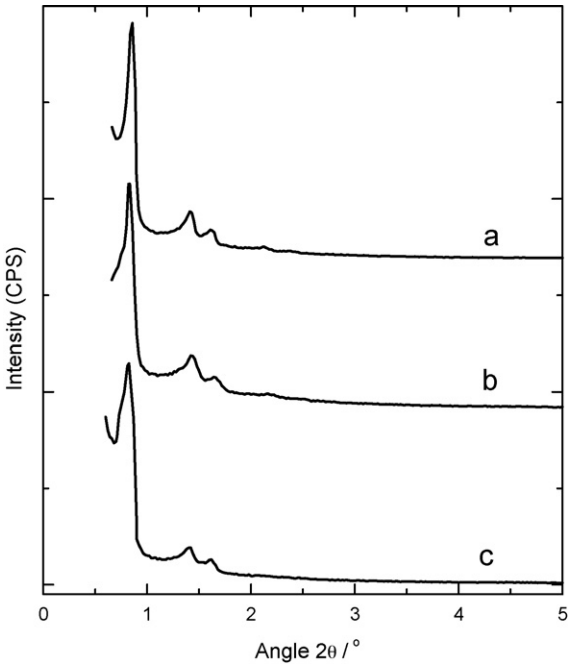

Fig. 1. XRD powder patterns of GaSBA-15 materials prepared at different n_{Si}/n_{Ga} ratios with $n_{H_2O}/n_{HCl} = 295$: (a) GaSBA-15(50), (b) GaSBA-15(15) and (c) GaSBA-15(10).

3.3. N_2 adsorption

The surface area, pore volume and pore size of calcined GaSBA-15 with various n_{Si}/n_{Ga} ratios are measured by N_2 adsorption isotherm (figure not shown). The textural properties of GaSBA-15 samples are given in Table 1. All isotherms are of type IV according to the IUPAC classification and exhibit a H1-type broad hysteresis loop, which is typical of large-pore mesoporous solids [20]. As the relative pressure increases ($p/p_0 > 0.6$), all isotherms exhibit a sharp step characteristic of capillary condensation of nitrogen within uniform mesopores, where the p/p_0 position of the inflection point is correlated to the diameter of the mesopore. Since SBA-15 has a hexagonal arrangement of mesopores connected by smaller micropores [21], it is clear that the broad hysteresis loop observed in the isotherms of GaSBA-15 reflects the long mesopores, which limit the emptying and filling of the accessible volume.

Table 1
Structural and textural parameters of GaSBA-15 materials prepared at different n_{Si}/n_{Ga} ratios

Sample	n_{H_2O}/n_{HCl}	n_{Si}/n_{Ga} ratio		Ga (wt%)	d_{100} (Å)	a_o (Å)	A_{BET} (m^2/g)	d_p (Å)	V_p (cm^3/g)	$t_w = a_o - d_p$ (Å)
		Gel	Calcined							
GaSBA-15(10)	295	10	12.7	0.342	107.1	123.7	981	88.4	1.08	35.3
GaSBA-15(15)	295	15	32.4	0.134	105.7	122.0	1007	87.7	1.07	34.3
GaSBA-15(25)	295	25	50.6	0.086	104.2	120.3	1038	86.8	1.05	33.5
GaSBA-15(50)	295	50	85.3	0.051	103.4	119.4	1068	86.2	1.04	33.2

Textural properties such as specific surface area, pore diameter, pore volume and pore wall thickness of GaSBA-15 samples systematically increase with decreasing n_{Si}/n_{Ga} ratios. GaSBA-15(10) has a lower specific surface area (981 m^2/g) but GaSBA-15(50) has a higher surface area (1068 m^2/g); however, the pore volume and pore wall thickness of the corresponding samples decrease from 1.08 to 1.04 cm^3/g and 35.3 to 33.2 Å, respectively. The pore diameter of GaSBA-15(10) is 88.4 Å, which is 2.2 Å higher than that of GaSBA-15(50). It is also interesting to note that the specific surface area, specific pore volume, pore diameter and pore wall thickness of GaSBA-15(10) are higher than those of other GaSBA-15 (Fig. 2) because GaSBA-15(10) has higher amount of Ga species than other GaSBA-15. Particularly, GaSBA-15 has higher pore diameter than SiSBA-15 because Ga–O has higher bond length than Si–O.

3.4. ^{71}Ga MAS NMR

Fig. 3 shows the ^{71}Ga MAS NMR spectra of calcined GaSBA-15 samples. The intensity of resonance peak increases, while the value of the chemical shift increases from 150 to 152 ppm with the increase of the amount of tetrahedral Ga^{3+} in the silica walls. Moreover, the peak width systematically is broadened with a higher Ga-ion content, indicating that Ga-ions are highly incorporated as coordinated tetrahedral Si^{4+} in calcined GaSBA-15. A resonance peak in this region has earlier been observed in other gallosilicate structure and is identified as originating from tetrahedrally-coordinated gallium present in the framework [22,23]. According to Bayense et al. [24,25], the concentration of tetrahedrally-coordinated gallium as the framework gallium can be measured by NMR reliably from the quantitative determination of the resonance peak area. However, a small amount of 6-coordinated gallium may also exist together with the 4-coordinated gallium although the relevant NMR peak (0 ppm) of the chemical shift of 6-coordinated gallium is invisible. Cheng et al. [26] also described that the concentration of 4-coordinated gallium can be estimated by ^{71}Ga NMR, indicating the possibility of finding tetrahedral-gallium. Hence, it can be concluded that the incorporation of gallium in the tetrahedral position of the MCM-41 or mesoporous structure can be achieved using ^{71}Ga MAS NMR.

The ^{71}Ga MAS NMR results reveal that the ''efficiency'' of Ga-ion incorporation increases when the n_{Si}/n_{Ga} ratios decrease from 85.3 to 12.7. These results are in good agreement with literature [23,26], where gallium is reportedly present as Ga^{3+}

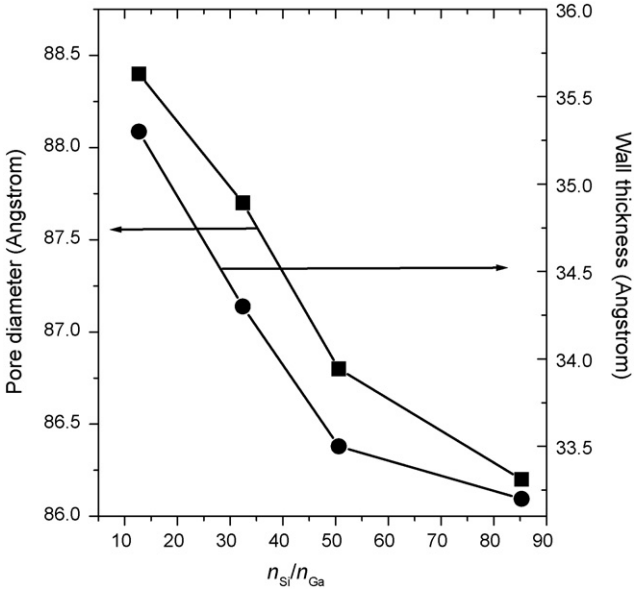

Fig. 2. Evaluation of unit cell parameter and wall thickness as a function of gallium nitrate content: (●) pore diameter and (■) wall thickness.

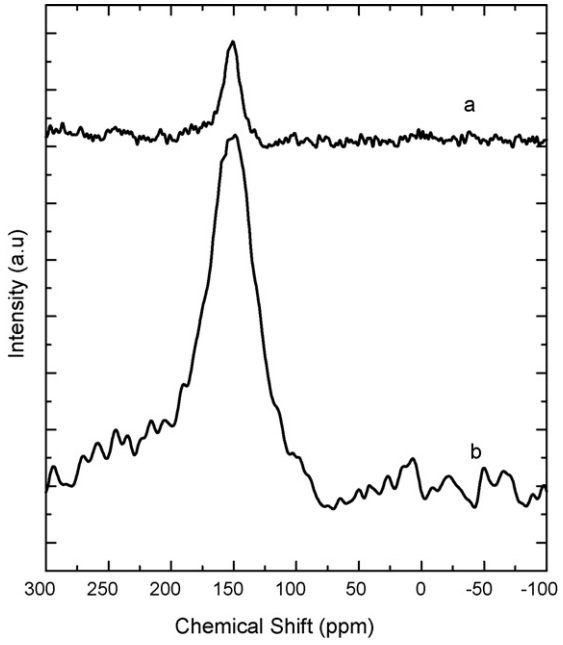

Fig. 3. ^{71}Ga MAS NMR spectra of calcined GaSBA-15 materials prepared at different n_{Si}/n_{Ga} ratios with $n_{H_2O}/n_{HCl} = 295$: (a) GaSBA-15(50) and (b) GaSBA-15(10).

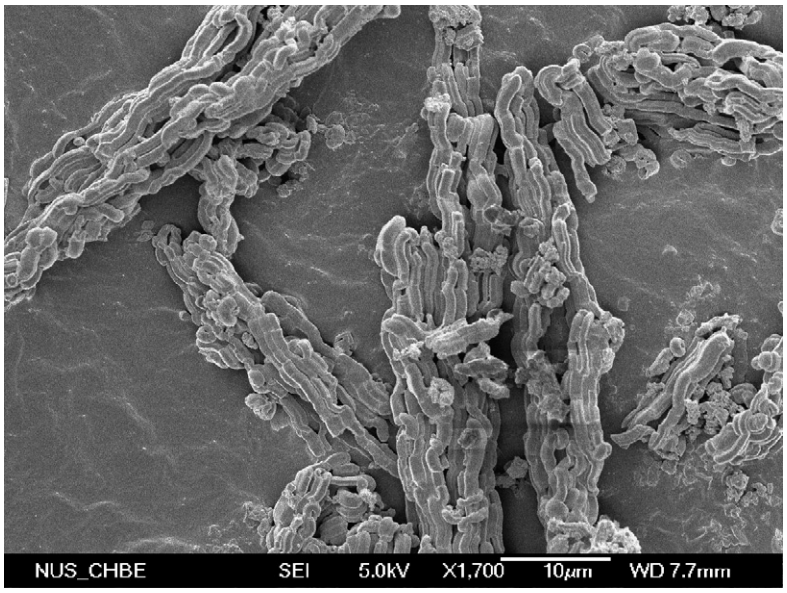

Fig. 4. Micrograph of calcined hexagonal mesoporous GaSBA-15(10).

ion in calcined GaSBA-15 samples, and most of Ga^{3+} ions are exclusively coordinated tetrahedrally to Si^{4+} on the silica pore walls. Furthermore, ^{29}Si MAS NMR studies show distinct signals at −111 and −110 ppm [26], which have been assigned to Q_4 and Q_3 (silicon) sites, respectively [26]. However, the signal of GaSBA-15 is weaker than siliceous SBA-15; this observation clearly supports the stabilization of gallium ions via silanol groups (defect sites).

3.5. FE-SEM and TEM

Fig. 4 shows a representative field emission-scanning electron microscopy image of mesoporous GaSBA-15(10). The morphology of GaSBA-15(10) can be controlled by the molar n_{H_2O}/n_{HCl} ratio of 295 in the synthesis gel at a fixed n_{Si}/n_{Ga} ratio to 10, with the resulting morphology as rope-like hexagonal mesoporous materials. GaSBA-15 material is made up of a bundle of ropes of diameter ∼12 μm and with a long rope-like aspect of as much as several hundred micrometers. It should be noted that the image of Fig. 4 is similar to that reported by Zhao et al. [17].

Fig. 5 shows the TEM image of GaSBA-15(10) sample. The TEM image shows well-ordered hexagonal arrays of 1D mesoporous channels, further confirming that GaSBA-15 sample has a 2D *p6mm* hexagonal structure. The distance between two consecutive centres of hexagonal pores estimated from the TEM image is ca. ∼11 nm. The average thickness of the wall is ca. ∼3.5 nm, which is much larger than that for MCM-41, and the pore diameter is around ∼8.8 nm, which is in agreement with the N_2 adsorption measurements.

3.6. t-Butylation of DHB

Acid-catalysed *t*-butylation is one type of Friedel–Crafts substitution reaction. Acidic mesoporous catalysts can catalyze such reaction due to the mild acidity of their protons. Because of the electrophilic nature of *t*-butylation over acidic catalysts, substitution at the *para*-position of DHB is favoured. The reaction products produced in this reaction are identified by GC/MS and ^1H NMR.

Mesoporous GaSBA-15 materials were tested as catalysts for selective *t*-butylation of DHB to TBC, which was carried out with isobutene/DHB molar ratio = 1 with 8.5 h^{-1} WHSV at 130 °C. This reaction also produces 3,5-DTBC (3,5-di-*t*-butylcatechol) as a major by-product and only traces amount of 3-TBC (*t*-butylcatechol) as minor by-product. Table 2 shows the catalytic activities of these GaSBA-15 catalysts, with the activity of the catalysts following this order: GaSBA-15(10) > GaSBA-15(15) > GaSBA-15(25) > GaSBA-15(50). Among these catalysts, GaSBA-15(10) exhibits the best performance, with DHB conversion of 93.2% and selectivity of 4-TBC around 95.7; these values are significantly higher than that of other GaSBA-15 catalysts under optimized reaction conditions. The observed higher activity of GaSBA-1(10) is probably attributed to its two-

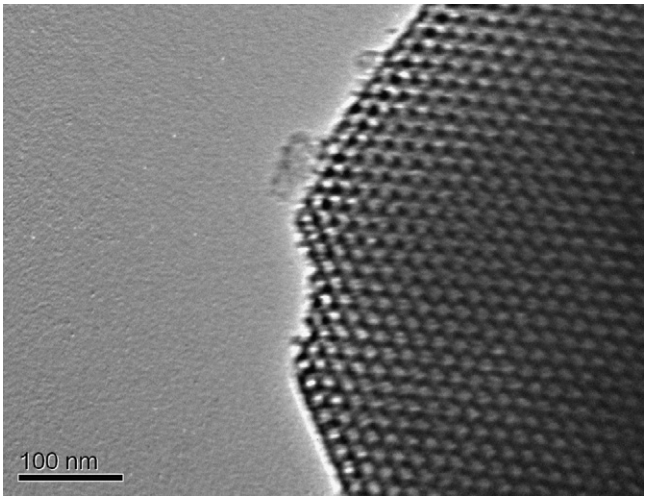

Fig. 5. TEM micrograph of calcined hexagonal mesoporous GaSBA-15(10).

Table 2
t-Butylation of DHB: variation of different catalyst

Catalysts	Conversion of DHB (%)	Product selectivity (%)		
		4-TBC	3,5-DTBC	3-TBC
GaSBA-15(10)	93.2	95.7	3.3	1.0
GaSBA-15(15)	86.6	90.4	8.5	1.1
GaSBA-15(25)	81.4	85.3	13.5	1.2
GaSBA-15(50)	77.1	80.3	18.3	1.4
GaSBA-15(10)-run1	93.2	95.7	4.3	–
GaSBA-15(10)-run2	92.9	95.4	4.3	0.3
GaSBA-15(10)-run3	92.9	95.6	4.3	0.1

Reaction conditions: Catalyst = 0.4 g; temperature = 130 °C; isobutene/DHB molar ratio = 1; WHSV = 8.5 h^{-1}; TOS = 3 h.

dimensional space and the high loading of tetrahedral Ga^{3+}on the inner pore structure framework, thus resulting in a higher number of accessible active sites because Ga^{3+}-ions produce a high number of Bronsted acid sites on the surface of pore walls. Based on these catalytic results, it is interesting to note that most of Ga^{3+}-ions might have been dispersed on the inner surface of the silica pore walls. Since GaSBA-15(10) is the most active catalyst, it is used further as the catalyst to search for the optimal reaction conditions of the *t*-butylation of DHB (such as temperature, WHSV, etc.).

For selective synthesis of 4-TBC over GaSBA-15(10), the performance of GaSBA-15(10) catalysts was investigated using different reaction conditions such as reaction temperature, WHSV, molar ratios of reactant (isobutene/DHB) and recyclability.

3.7. Effect of reaction temperature

The *t*-butylation of DHB was carried out under various reaction temperatures using isobutene/DHB molar ratio = 1 and WHSV = 8.5 h^{-1} over GaSBA-15(10) catalyst. The effect of reaction temperature in the range 100–180 °C on the activity and selectivity is exhibited in Fig. 6. Basically, DHB conversion increases with increasing reaction temperature from 100 to 180 °C. Although the selectivity of 4-TBC increases with increasing reaction temperature from 100 to 130, however at higher reaction temperature (above 140 °C), the selectivity decreases due to the increase of the amount of 3,5-DTBC in the reaction products because once 4-TBC is formed, 4-TBC reacts with isobutene to form 3,5-DTBC. Therefore, the formation of 4-TBC is favoured at lower reaction temperature. The selectivity of 3-TBC shows an inverse trend compared to that of 3,5-DTBC as 3-TBC is also formed at lower temperature and its selectivity almost remains constant at higher temperature up to 180 °C. Based on these results, the proper reaction temperature is chosen to be about 130 °C for optimal DHB conversion and 4-TBC selectivity.

3.8. Effect of WHSV

Fig. 7 shows the effect of the space velocity of the feed on the catalytic properties of GaSBA-15(10) catalyst, while the reaction was carried out under various WHSV at 130°C using isobutene/DHB molar ratio = 1 over GaSBA-15(10). Although the conversion of DHB slowly decreases with increasing WHSV from 8.5 to 42.5 h^{-1}, however the selectivity of 4-TBC remains constant. At high WHSV (17–42.5 h^{-1}), the selectivity of 3,5-DTBC is slightly reduced with the slight increase of 3-TBC due to the shorter contact time. The optimal WHSV for high selectivity of 4-TBC with good conversion of DHB is 8.5 h^{-1}.

3.9. Effect of isobutene to DHB molar ratios

Fig. 8 shows the conversion of DHB and the selectivity of 4-TBC of *t*-butylation of DHB under different isobutene/DHB molar ratios with 8.5 h^{-1} WHSV at 130 °C over GaSBA-15(10). The conversion of DHB and the selectivity of 4-TBC increase with increasing isobutene/DHB molar ratios from 0.6 to 1. However, when isobutene/DHB molar ratio is further increased >1, the conversion of DHB increases but the

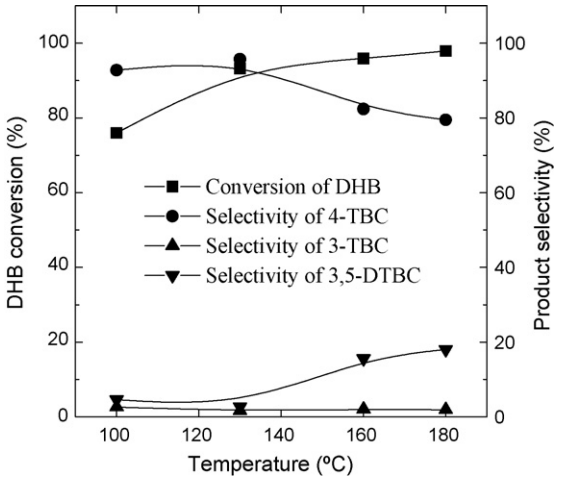

Fig. 6. Variation of conversion of DHB (%) and product selectivity (%) with reaction temperature over GaSBA-15(10) (reaction conditions: catalyst = 0.4 g; isobutene/DHB molar ratio = 1; WHSV = 8.5 h^{-1}).

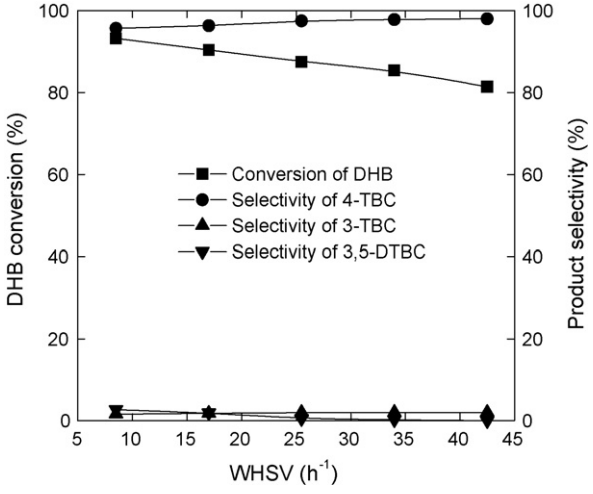

Fig. 7. Variation of conversion of DHB (%) and product selectivity (%) with WHSV over GaSBA-15(10) (reaction conditions: catalyst = 0.4 g; temperature = 130 °C; isobutene/DHB = 1).

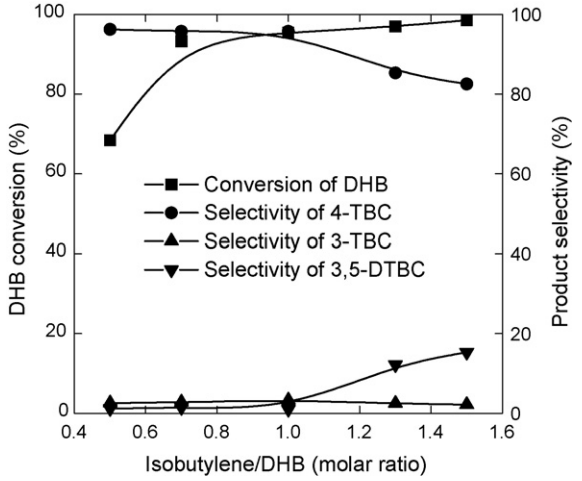

Fig. 8. Variation of conversion of DHB (%) and product selectivity (%) with feed molar ratio over GaSBA-15(10) (reaction conditions: catalyst = 0.4 g; temperature = 130 °C; WHSV = 8.5 h^{-1}).

selectivity of 4-TBC decreases due to the increase of 3,5-DTBC selectivity. Based on these results, the selectivity of 4-TBC is higher in isobutene/DHB molar ratio = 1 as compared to that of other molar ratios.

3.10. Effect of TOS and recyclability

The catalytic performance of GaSBA-15(10) has been investigated under different TOS (time on steam) for *t*-butylation of DHB with isobutene/DHB molar ratio = 1 and 8.5 h^{-1} WHSV at 130 °C. The DHB conversion increases from 64% to 76% in 2 h and then from 76% to 93.2% in 3 h; after that, it remains almost constant up to 10 h. But the selectivity of 4-TBC and 3,5-DTBC slightly increases with time on stream. The selectivity of 4-TBC increases with increasing concentration of DHB, and the selectivity of 3,5-DTBC increases when the increased concentration of isobutene reacts with 4-TBC. Therefore, the deactivation of catalyst has not taken place during the course of study (figure not shown).

One of the essential advantages of using solid catalyst for vapour phase reaction is the easy regeneration of the catalyst from the unreacted reactants and products. The repeated use of GaSBA-15 catalyst has been investigated at 130 °C. The first run gave 95.7% 4-TBC selectivity at 93.2% DHB conversion. The used catalyst was calcined at 500 °C in air and then reused again in the second run of the reaction. The same procedure was repeated for the third run and the results are shown in Table 2. The conversion of DHB and the selectivity of 4-TBC remain essentially constant even after three cycles, showing that GaSBA-15 is a potential commercial catalyst for the *t*-butylation of DHB to 4-TBC.

4. Conclusions

Mesoporous GaSBA-15 material has been successfully synthesised using pH-adjusting method to incorporate a high amount of Ga-ions into the mesoporous framework of SBA-15 without destroying the mesoporous structural order. ICP-AES results show that there is a high amount of Ga species incorporated into the framework of SBA-15. XRD and N_2 adsorption studies show that the structural and textural properties of GaSBA-15 could be improved due to the incorporation of a high amount of Ga-ions on the silica walls. ^{71}Ga MAS NMR studies confirm that the Ga^{3+} species is incorporated with tetrahedral coordination. FE-SEM and TEM images confirm that the GaSBA-15 catalyst has a long rope-like morphology and uniform pore diameter. In order to obtain the maximum conversion of DHB conversion and the highest selectivity of 4-TBC, the *t*-butylation of DHB reaction should be carried out over GaSBA-15(10) catalyst at 130 °C and WHSV of 8.5 h^{-1} under a molar ratio of isobutene/DHB = 1. Furthermore, GaSBA-15(10) catalyst can be recycled at least three times without losing its catalytic performance, showing that it has the potential commercial application as the selective alkylation catalyst.

Acknowledgment

The Singapore Millennium Fellowship (SMF) awarded by the Singapore Millennium Foundation for M. Selvaraj (2005-SMF-0437) is gratefully acknowledged for this work.

References

[1] R.E. Burk, Twelfth Catalyst Report, National Research Council, Wiley, New York, 1940, p. 266.
[2] J. Nagaoka, Jap. Patent 49,109,325 (1974).
[3] S.-E. Park, J.W. Yoo, C.W. Lee, Y.K. Park, J.-S. Chang, Y.C. Lee, K.S. Choi, Korean Patent Appl. 9,857,206 (1998).
[4] S.-E. Park, C.W. Lee, J.W. Yoo, Y.C. Lee, H.-C. Jeong, Korean Patent Appl. 9,945,641 (1999).
[5] T.P. Malloy, D.J. Engel, US Patent 4,323,714 (1982).
[6] A. Corma, A. Martinez, Catal. Rev. Sci. Eng. 35 (1993) 483.
[7] J.W. Yoo, D.S. Kim, J.-S. Chang, S.-E. Park, Stud. Surf. Sci. Catal. 105 (1997) 2035.
[8] H. van Bekkum, Stud. Surf. Sci. Catal. 41 (1988) 23.
[9] S.-J. Chu, Y.-W. Chen, Appl. Catal. A 123 (1995) 51.
[10] G. Bellussi, G. Pazzuconi, C. Perego, G. Girotti, G. Terzoni, J. Catal. 157 (1995) 227.
[11] J. Cejka, N. Zilkova, B. Wichterlova, G. Eder-Mirth, J.A. Lercher, Zeolites 17 (1996) 265.
[12] (a) J.W. Yoo, C.W. Lee, S.-E. Park, J. Ko, Appl. Catal. A 187 (1999) 225; (b) R. Anand, R. Maheswari, K.U. Gore, V.R. Chumbhale, Catal. Commun. 3 (2002) 321; (c) J.W. Yoo, C.W. Lee, H.-C. Jeong, Y.K. Park, S.-E. Park, Catal. Today 60 (2000) 255.
[13] Y. Ono, Stud. Surf. Sci. Catal. 5 (1980) 19.
[14] C.T. Kresge, M.E. Leonowicz, W.J. Roth, J.C. Vartuli, J.S. Beck, Nature 359 (1992) 710.
[15] J.S. Beck, J.C. Vartuli, W.J. Roth, M.E. Leonowicz, C.T. Kresge, K.D. Schmitt, C.T.-W. Chu, D.H. Olson, E.W. Sheppard, S.B. McCullen, J.B. Higgins, J.L. Schlenker, J. Am. Chem. Soc. 114 (1992) 10834.
[16] M. Selvaraj, B.H. Kim, J. Han, T.G. Lee, Stud. Surf. Sci. Catal. 156 (2005) 803.
[17] D. Zhao, J. Feng, Q. Huo, N. Melosh, G.H. Fredrickson, B.F. Chmelka, G.D. Stucky, Science 279 (1998) 548.
[18] (a) J.J. Chiu, D.J. Pine, S.T. Bishop, B.F. Chmelka, J. Catal. 221 (2004) 400; (b) Y. Sun, S. Walspurger, J.P. Tessonnier, B. Louis, J. Sommer, Appl. Catal. A: Gen. 300 (2006) 1; (c) Z. El Berrichi, B. Louis, J.P. Tessonnier, O. Ersen, L. Cherif, M.J. Ledoux, C. Pham-Huu, Appl. Catal. A: Gen. 316 (2007) 219;

(d) B. Jarry, F. Launay, J.P. Nogier, V. Montouillout, L. Gengembre, J.L. Bonardet, Appl. Catal. A: Gen. 309 (2006) 177;
(e) Z. El Berrichi, L. Cherif, O. Orsen, J. Fraissard, J.P. Tessonnier, E. Vanhaecke, B. Louis, M.J. Ledoux, C. Pham-Huu, Appl. Catal. A: Gen. 298 (2006) 194.
[19] M. Selvaraj, S. Kawi, Chem. Mater. 19 (2007) 509.
[20] A. Sayari, P. Liu, M. Kruk, M. Jaroniec, Langmuir 13 (1997) 2499.
[21] M. Imperor-Clerc, P. Davidson, A. Davidson, J. Am. Chem. Soc. 122 (2000) 11925.
[22] H.K.C. Timken, E. Oldfield, J. Am. Chem. Soc. 109 (1987) 7669.
[23] M. Chatterjee, T. Iwasaki, Y. Onodera, T. Nagase, H. Hayashi, T. Ebina, Chem. Mater. 12 (2000) 1654.
[24] C.R. Bayense, J.H.C. van Hooff, A.P.M. Kentgens, J.W. de Hann, L.J.M. van de Van, J. Chem. Soc., Chem. Commun. (1989) 1292.
[25] C.R. Bayense, A.P.M. Kentgens, J.W. de Hann, L.J.M. van de Van, J.H.C. van Hooff, J. Phys. Chem. 96 (1992) 775.
[26] C. Cheng, H. He, W. Zhou, J. Klinowski, J.A.S. Goncalves, L.F. Gladden, J. Phys. Chem. 100 (1996) 390.